RESEARCH ARTICLE   OPEN ACCESS

Analysis and performance evaluation of FPGA controlled Resonant Converter for heating application

N.Soundiraraj, Dr V.Rajasekaran

[1]Assistant professor, ,[2] Professor& Head

[1,2] (Electrical and Electronics Engineering, PSNA College of engineering and technology,Dindigul)

Abstract:

Resonant power converters are widely used due to their advantages in terms of size, efficiency, and power density. One of the main design difficulties derives from the need to accurately tune the resonant tank and the operating conditions to achieve the desired performance. This is especially challenging in those applications in which either the resonant tank or the operating conditions are highly variable. This paper proposes and compares several implementations of online parametric identification algorithms to identify the resonant tank of power converters taking advantage of field-programmable gate array technology. The proposed implementations are based on the phase-sensitive detector algorithm, which ensures an accurate harmonic identification of the resonant load. The proposed identification system is tested using a resonant power converter prototype applied to induction heating systems, proving the feasibility and accuracy of this proposal.

Keywords — Embedded systems, field-programmable gate arrays (FPGAs), induction heating (Electrical heating), resonant power conversion.

I.INTRODUCTION

I N RECENT years, the market of domestic electrical heating cook tops has been growing due to the fact that electrical heating technology offers safety, cleanness, and higher efficiency when compared with the classical heating systems [1]–[3]. An exploded view of a domestic electrical heating cooktop is displayed in Fig. 1(a) showing all of the main components. The power conversion scheme of an electrical heating Hob is shown in Fig. 1(b). The inverter stage commonly features resonant power converter architectures to achieve efficient and compact implementations. In this paper, the half-bridge topology has been chosen because of its good cost/performance balance.

Fig. 1. Domestic induction cooktop: (a) exploded view and (b) general block diagram.

This inverter topology can deliver a wide range of power, usually between 50 W and 3.5 kW. The inductor–vessel system is part of the inverter resonant tank. Hence, this impedance sets the inverter operating point and the safe operating area. Usually, the electrical load impedance is modelled as an equivalent series L-R circuit. [4]–[6]. Moreover, this impedance depends on several parameters such as geometry, frequency, or temperature; and it may vary during the inverter operation. Because of this and the wide output power range, the inverter operating conditions are highly variable [7], [8]. Thus, an online impedance identification system is desirable to ensure the reliability and proper inverter operation. Moreover, this system can help the control system to improve the dynamic behavior of the power converter [3], [9]–[11] and to minimize the output power overshoots typical in domestic electrical heating application due to the vessel movements. In addition to this, the online impedance identification is mandatory to implement some required security tasks such as vessel removal detection. Generally, identification algorithms are classified into non parametric and parametric methods [12], [13]. Non parametric methods calculate directly the system frequency response making no assumption about the system structure. Parametric methods estimate the model parameters of an assumed system model [14]. In the literature, several parametric algorithms applied to the domestic electrical heating application have been presented. In [15], a small signal load characterization is performed using a commercial impedance analyzer. However,
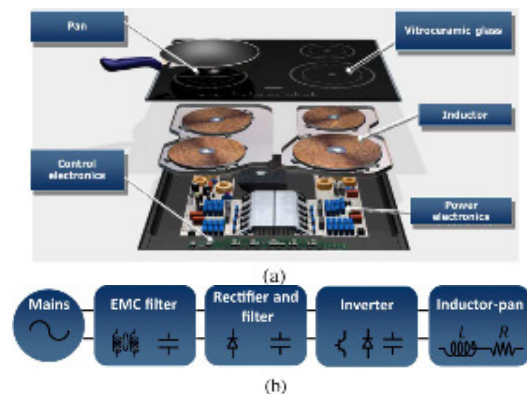
the small-signal characterization is not sufficient for electrical heating application due to nonlinear effects. To identify the induction load while operating under real conditions, in [16] and [17], two large-signal identification test-benches are presented. However, both of them use offline identification methods, making them unfeasible for closed-loop control. In [18] and [19], online large-signal identification systems based on the discrete-time Fourier series calculation are presented. Nevertheless, due to phase errors, the accuracy of these systems is not sufficient to perform some security tasks, which require 2.5% accuracy. Finally, in [20], an online identification system based on the PSD algorithm [21] is proposed. This paper proposes an online large-signal parametric identification method for identifying the resonant tank impedance of domestic electrical heating systems. To comply with the electrical heating application requirements, the proposed identification algorithm is based on the PSD algorithm. The proposed system takes advantage of FPGA technology [22]–[24], which has significantly increased performance and decreased cost, making them interesting for industrial applications [25]–[28], including real-time identification systems [29]. The system presented in [20] has been extended to cover a rectified ac power supply. Moreover, a second-order 1-bit $\sum\Delta$.ADC specifically designed for the electrical heating application has been used [24]. Taking the advantage of this ADC architecture, the PSD hardware resources consumption is minimized by applying the PSD algorithm directly to the 1-bit ADC output. An analysis of several PSD implementations is provided, which is key for this application. Finally, a calibration process is performed while working under real operating conditions to assess the system accuracy and additional experimental results while working with several commercial vessels have been included.

This paper is structured as follows. Section II details the identification algorithm proposed in this paper. Section III analyzes and optimizes the design for the Electrical heating application and Section IV details the digital system implementation in an FPGA. Section V performs the calibration of the identification system and analyzes its accuracy, and Section VI verifies the identification system working with actual Electrical heating loads. Finally, Section VII summarizes the conclusion of this paper.

II. LOCK-IN PARAMETRIC IDENTIFICATION ALGORITHM

PSD, also called lock-in amplifier, is a tool that allows accurate measurement of the signals for a defined frequency even when the signal is highly buried in noise. The identification algorithm selected in this paper uses the PSD system for extracting the equivalent series Resistor-Inductor-Capacitor (RLC) circuit parameters of the inverter resonant tank. The capacitance of this circuit is due to the resonant capacitor Cr and the RL circuit belongs to the inductor–vessel model. The equivalent inductor–vessel circuit Rh-Lh at the n

th harmonic is calculated from the digitized voltage and current applied to the RLC circuit,Vo and I_L , respectively. This identification process is divided into two tasks. First, the h th harmonic components of the voltage Voh and the current ILh are computed using two PSD systems. Second, the impedance is computed from the PSD results.

THE PHASE SENSITIVE DETECTOR(PSD)
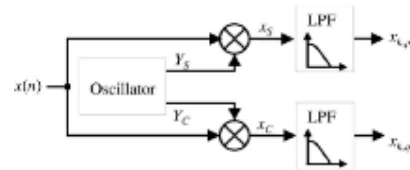
The PSD block diagram is shown in Fig. 2 [20], [21].

Fig. 2. PSD block diagram.

The PSD input is multiplied by two sine wave signals in quadrature, Ys and Yc , with the same frequency as the h th harmonic:Due to finite precision implementation effects, the oscillator can generate only a finite number of frequencies; Then, two LPFs filter the Xs and Xc signals to eliminate the high-frequency components. The filter outputs are the in-phase and quadrature components of the input.

B. Impedance Measurement

To measure the load impedance, the voltage applied to the RLC circuit and the inductor current is digitalized by two ADCs. Afterward, the equivalent impedance of the resonant tank,

$$Z = V/I$$

III. ANALYSIS AND DESIGN OPTIMIZATION

The identification system will be implemented in the control system of a domestic electrical heating appliance. In this paper, it has been considered a control system based on a hardware software code sign using a microprocessor and digital hardware. This section analyzes and designs the identification algorithm applied to this application.

A. Inverter Topology

Fig. 3 shows the half-bridge topology (a), the inverter bus voltage (b), and the inverter modulation parameters and main waveforms (c). The switching frequency is controlled within the range from 30 to 80 kHz. The period of the input voltage is half of the mains period. The control algorithm is executed at the zero-crossing of the mains voltage;   the control algorithm computes the modulation parameter values for the next half-main cycle. Thus, the control system requires one impedance measurement each
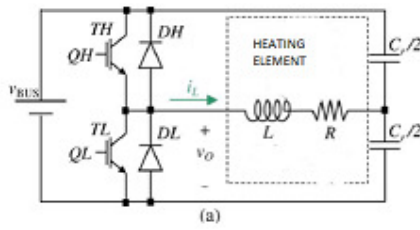
Fig. 3. Resonant inverter: (a) half-bridge schematic circuit, (b) inverter bus voltage, and (c) modulation parameters.
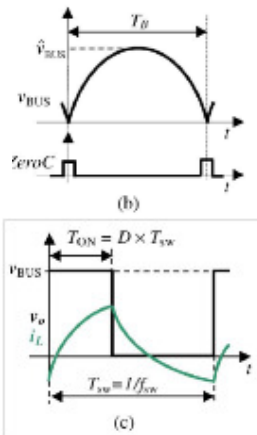

Fig. 3. Resonant inverter: (a) half-bridge schematic circuit, (b) inverter bus voltage, and (c) modulation parameters.
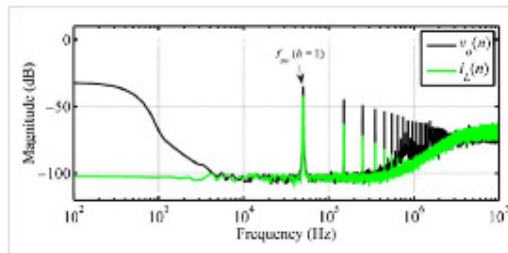

Fig. 4. Power spectrum density estimation of the digitized signals.

B. Measurement Circuit

The most important advantages of these converters from the point of view of this application are the low cost and the easy integration in an Application-Specific Integrated Circuit (ASIC). Fig. 4 shows the power spectrum density estimation of the digitized signals. The output voltage also contains the dc component.

C. PSD: Oscillator Considerations

The PSD detector computes digitally the h harmonic in phase and quadrature components of the input signal (Fig. 2). The accuracy in the harmonic components depends on the

reference signals quality and the effectiveness of the filter to remove the undesired frequencies. Several digital architectures for generating the reference sine wave signals have been proposed in the literature. The NCO architectures store the sine samples in a look-up table and read these samples at constant time intervals. In [30], an assortment of NCO schemes is given. Another option for implementing two quadrature sine waves is by using a coupled recursive oscillator [31]. These oscillators compute a second-order difference equation whose characteristics roots are on the unit circle in the plane. The main drawback of these structures is the stability problems associated with the finite word-length effects, which causes amplitude and frequency deviations. However, in literature, several control methods have been proposed for minimizing, or even eliminating, the amplitude and frequency deviations [32]. Besides, coupled oscillators are more flexible and use less hardware resources than NCOs.the reference signal frequency is equal to the desired one .

D. PSD: LPF Filter Design

A considerable amount of literature has been published proposing the different implementations of digital filters. The digital filters, according to its unit impulse response, are classified into two groups: FIR and IIR. The main advantage of the linear-phase FIR filters compared to the IIR filters is that they maintain the waveform of the in-band signal components. However, as the filter specifications become more restrictive, the complexity of the FIR filters arises in comparison with the complexity of the IIR counterparts. In order to reduce the complexity of the filter and digital resources needed, multi-rate filtering techniques are used [33]. The multi-rate technique changes the sampling rate of the input signal in order to relax the filter specifications. The specifications for the LPFs are fixed by the modulation parameters of the power inverter and the ADC converter.
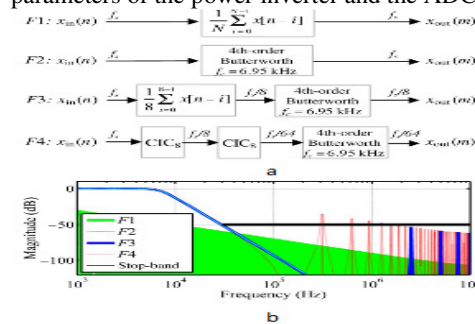

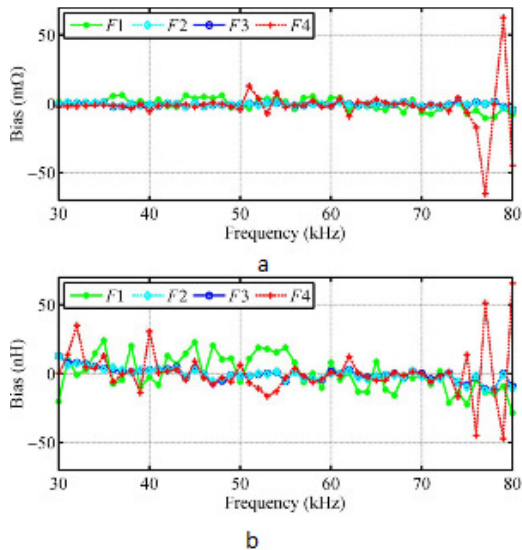Fig. 5. Analyzed filters: (a) filter architectures and (b) frequency response.

Fig. 6. Simulation results of the first-harmonic impedance measurements for ideal oscillator: (a) bias of resistance R and (b) bias of inductance L . variety of filter architectures proposed in the literature, the filters shown in Fig. 5(a) have been selected to be analyzed. Taking into account the simulation results, two implementations of the LPFs have been selected to be experimentally verified: the filter F1 as a cost-effective solution and the filter F3 as a trade-off between the cost and performance.

IV. DIGITAL IMPLEMENTATION

The identification system has been designed to be implemented in a hardware–software co-design control system embedded in an FPGA [34]. The output voltage and current PSD blocks have been implemented in hardware The identification algorithm has been tested in a Spartan-6 FPGA from XILINX, Fig. 8 details the digital subsystem block diagram, which consists of two platforms: Hardware Platform and Software Platform.
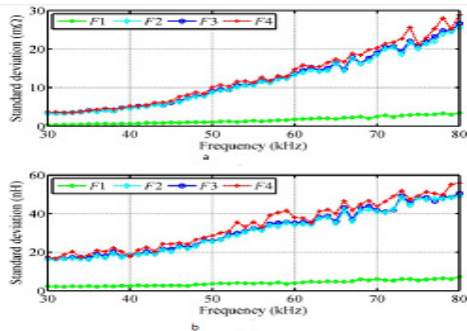

Fig.7. Simulation results of the first-harmonic impedance measurements for ideal oscillator: (a) standard deviation of resistance Rand (b) standard deviation of inductance L
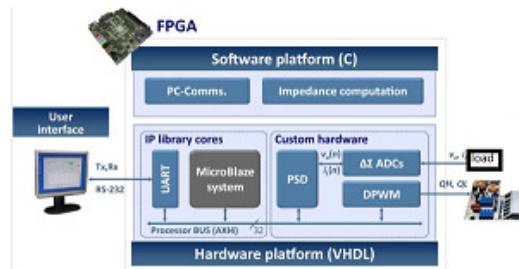

Fig. 8. Digital system block diagram

A. Hardware Platform

The hardware platform is made up of the MB system and several custom peripherals. These peripherals are attached to the microprocessor system through the processor local bus AMBAAXI4. The microprocessor system has been built using intellectual property (IP) cores provided by XILINX and includes the Micro Blaze core, data and instruction memories, interrupt controller, and watchdog. In order to establish communication with the user interface, it has been included a communication IP core (UART). The digital subsystems that perform specific tasks have been described inVHDL hardware description language, and are composed of the peripherals DPWM and PSD. The DPWM peripheral generates the gating signals that control the half-bridge modulation. The ADCs block includes the digital elements of the ADCs. Finally, the PSD block implements the PSDs of the identification method (Fig. 2). In order to minimize the required digital resources and the spurious components, the standard quadrature coupled oscillator [31] has been selected for generating the PSD reference signals. Table I summarizes the logic resources required to implement each block in a Xilinx Spartan-6 XC6SLX45 FPGA. The final identification system will implement one oscillator, which generates the reference signals of the two PSD, four multiplications and four filters

B. Software Platform

This platform contains the C-language program executed by MicroBlaze. This software performs two main tasks: impedance computation and communication with the user interface. The impedance computation algorithm calculates the impedance of the load by using (6) and (7) in float-point format. This calculus is done when the signal Zero Crossing is activated, i.e., each

10 Mrs. Therefore, the timing constraints to perform this task are not restrictive. Moreover, the software implementation of such equations allows adapting the identification algorithm to the

system parameters such as the conditioning circuit values Rm and Av The algorithm computes two impedances, one for each

TABLE I
DIGITAL IMPLEMENTATION FOR THE PSD BLOCK

Digital resources	Oscillator	Mult.	F1	F3	Available
Slice registers	64	0	64	340	54 576
Slice LUTs	119	20	33	342	27 288
DSP48A1s	4	0	0	8	58

filter implemented in the LPF blocks, i.e.,F1 and F3 . Thus, the results in the impedance measurement for both filters can be compared. The PC-Comms. routine establishes a serial RS-232 communication with the graphical user interface. This routine allows configuring the reference signals frequency and the modulation parameters of the power inverter. It also allows retrieving the impedance measurements.
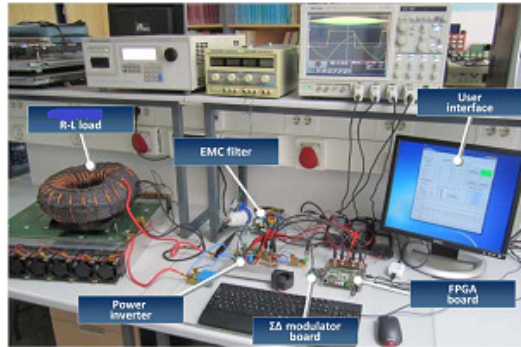

Fig. 10. Experimental prototype

VI. EXPERIMENTAL RESULTS

The implemented system, i.e., approach F1 , has been verified while working under real operating conditions with several electrical heating loads. The commercial vessels used in the experimental verification are: a ferromagnetic pot, a multilayered pot, and an enameled pot. Fig. 11 shows the results of the impedance identification for these vessels versus the switching frequency. The frequency ranges of the measurements are determined by the power delivered to the vessels. These ranges cover from the maximum switching frequency, i.e., minimum power, up to 2500Wapproximately. In order to avoid temperature influence, these measurements have been performed with boiling water. The impedance variation shown in this figure highlights the need of a real-time impedance measurement system and proves the feasibility of the proposed system. Fig. 12 shows the real-time impedance measurements for the same vessels during the heating of 1.5 l of water from 25 degree celcius to boiling temperature. During this experimental test, the switching frequency is fixed to 50 kHz. The graphs show the influence of the load impedance versus the temperature. As the temperatures of the vessels increase, so do their equivalent inductance and resistance. When the load temperatures stabilize at 100 , i.e., the water starts boiling, the load impedances also stabilize. This graph shows that, although the switching frequency is the same for all
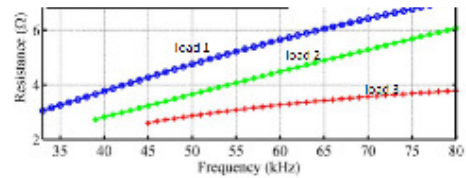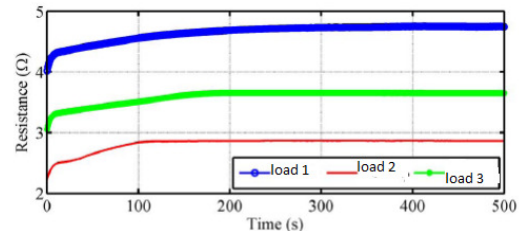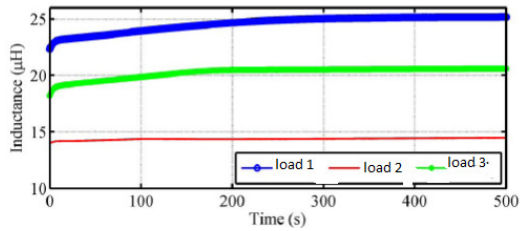

(a)
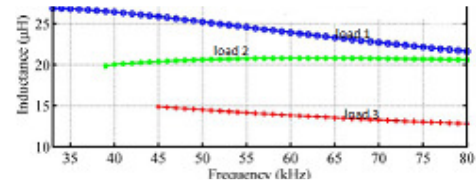
(b)

Fig. 11. Experimental results of first-harmonic impedance measurement for different commercial electrical load versus switching frequency: (a) equivalent resistance R1 and (b) equivalent inductance L1

(a)

(b)

Fig. 12. Real-time measurements of first-harmonic impedance measurement for different loads during heating (a) equivalent resistance R1 and (b) equivalent inductance L1.

VII. CONCLUSION

In this paper, a digital system for measuring the load impedance of resonant inverters online has been proposed. The identification system has been applied to a electric heating system, which implements a hardware–software co-design control system based on a microprocessor and an ASIC. The implemented algorithm uses the PSD (lock-in) system to obtain the in-phase and quadrature components of the resonant power converter output voltage and current. From these

components, the values of the equivalent circuit of the electrical load system are computed. The measurement method has been analyzed and several architectures for the PSD system have been verified through simulation. Two of these implementations have been experimentally tested. The experimental verification shows that the error in the first harmonic resistance and inductance measurements is lower than 1%. The obtained accuracy meets the Electrical heating application requirements. Finally, the proposed online impedance measurement system can help the control system to improve the dynamic performance of the power converter by adapting the controller to the actual electrical load, and to assure the safe converter operation by performing some security tasks, for instance, load detection and soft-switching conditions verification. This is mandatory in the Electrical heating application because of its highly variable resonant tank impedance and operating conditions.

REFERENCE

[1] O.Lucia,J.Acero,C. Carretero, and J. M. Burdío, "Induction heating appliances: Towards more flexible cooking surfaces," IEEE Ind. Electron. Mag., vol. 7, no. 3, pp. 35–47, Sep. 2013.

[2] O. Lucía, P. Maussion, E. Dede, and J. M. Burdío, "Induction heating technologyanditsapplications:Pastdevelopments,currenttechnology,and future challenges," IEEE Trans. Ind. Electron., vol. 61, no. 5, pp. 2509–2520, May 2014.

[3] O. Lucía, I. Cvetkovic, H. Sarnago, D. Boroyevich, P. Mattavelli, and F.C. Lee, "Designofhome appliancesfor adc-basednanogridsystem:An inductionrangestudycase,"IEEEJ.Emerg.Sel.TopicsinPowerElectron., vol. 1, no. 4, pp. 315–326, Dec. 2013.

[4] J. Acero, C. Carretero, R. Alonso, O. Lucía, and J. M. Burdío, "Mutual impedance of small ring-type coils for multi-winding induction heating appliances," IEEE Trans. Power Electron., vol. 28, no. 2, pp. 1025–1035, Feb. 2013.

[5].C.Carretero,O.Lucía,J.Acero,R.Alonso,andJ.M.Burdío,"Frequencydependentmodelingofdomesticinductionheatingsystemsusingnumerical methodsforaccuratetime domainsimulation,"IETPowerElectron.,vol.5, no. 8, pp. 1291–1297, Sep. 2012.

[6] S. Chudjuarjeen, A. Sangswang, and C. Koompai, "An improved LLC resonant inverter for induction-heating applications with asymmetrical control," IEEE Trans. Ind. Electron., vol. 58, no. 7, pp. 2915–2925, Jul. 2011.

[7] H. Sarnago, O. Lucía, A. Mediano, and J. M. Burdío, "Design and implementation of a high-efficiency multiple-output resonant converter for induction heating applications featuring wide bandgap devices," IEEE Trans. Power Electron., vol. PP, no. 99, p. 1, Aug. 2013.

[8]H.Sarnago,O.Lucía,A.Mediano,andJ.M.Burdío,"Directac–acresonant boost converter for efficient domestic induction heating applications," IEEE Trans. Power Electron., vol. 29, no. 3, pp. 1128–1139, Mar. 2014.

[9] H. N. Pham, H. Fujita, K. Ozaki, and N. Uchida, "Dynamic analysis and control for resonant currents in a zone-control induction heating system," IEEE Trans. Power Electron., vol. 28, no. 3, pp. 1297–1307, Mar. 2013.

[10]W.Feng,F.C.Lee,andP.Mattavelli,"Simplifiedoptimaltrajectorycontrol (SOTC) for LLC resonant converters," IEEE Trans. Power Electron., vol. 28, no. 5, pp. 2415–2426, May 2013.

[11]W.Feng,F.C. Lee, and P. Mattavelli, "Optimal trajectory control of burst mode for LLC resonant converter," IEEE Trans. Power Electron., vol. 28, no. 1, pp. 457–466, Jan. 2013.

[12] L. Ljung, System Identification: Theory for the User, 2nd ed., Englewood Cliffs, NJ, USA: Prentice-Hall, 1999.